Available online at www.sciencedirect.com
SCIENCE DIRECT
Catalysis Today 107–108 (2005) 46–52
CATALYSIS TODAY
www.elsevier.com/locate/cattod

Carbon-supported platinum-molybdenum electro-catalysts for methanol oxidation

L.C. Ordóñez [a], P. Roquero [b,*], P.J. Sebastian [a], J. Ramírez [b]

[a] *Centro de Investigaciones en Energía—Universidad Nacional Autónoma de México, CP 62580 Temixco, Morelos, México*
[b] *Unidad de Investigación en Catálisis, Facultad de Química—Universidad Nacional Autónoma de México, CP 04510 México D.F., México*

Available online 19 August 2005

Abstract

The synthesis and characterization of catalysts based on bimetallic materials, Pt–Mo supported on carbon for the anodic oxidation of methanol in direct methanol fuel cells is reported here. The catalysts were synthesized from the Pt carbonyl complex ($[Pt_3(CO)_3\ (\mu_2\text{-}CO)_3]_n^{2-}$), prepared by bubbling CO through a chloroplatinic acid solution. The supported Pt–Mo/C materials were prepared in a reflux system, by mixing different amounts of Mo hexacarbonyl complex, Pt–carbonyl complex and carbon, using *o*-xylene as solvent. The Pt–Mo/C materials were characterized by cyclic voltammetry (CV) in methanol, formaldehyde and formic acid solutions with H_2SO_4 as supporting electrolyte. Rotating disk electrode (RDE) voltammetry tests were carried out to determine the electric potentials in which the electrode reactions involve a diffusion process. The highest activity towards anodic methanol oxidation was obtained with materials with low molybdenum loadings.

Keywords: Anodic methanol oxidation; Electrocatalysis; Platinum; Molybdenum; Carbon-supported catalyst

1. Introduction

Fuel cells are devices in which electric power is produced directly from electrochemical reactions with low pollutant emissions, and higher efficiency than internal combustion operating systems. Methanol is easy to be stored and transported, and has higher energy density with respect to hydrogen. For this reason it has been considered as a viable fuel to be used in fuel cells for mobile applications and portable power units. Systems operated with this alcohol are named direct methanol fuel cells (DMFC), since this compound is fed directly to the system in gas or liquid form. The DMFC consists of an anode at which methanol is electro-oxidized to CO_2 and a cathode where oxygen, generally from air, is reduced to form water. Both electrodes, usually formulated with platinum, are separated by a proton-conducting electrolyte.

The overall methanol oxidation reaction occurring at the anode is:

$$CH_3OH + H_2O \rightarrow CO_2 + 6H^+ + 6e^-$$

For this reaction, the standard equilibrium potential is $E^0 = 0.046$ V versus reversible hydrogen electrode (RHE). However, the transfer of the six electrons in this reaction occurs with the formation of several intermediate species such as CO, $(CH_xOH)_{ad}$, formyl $(–COH)_{ad}$, carboxyl $(–COOH)_{ad}$ or formic acid dimmers $(HCOOH)_{2ad}$ [1–3], which adsorb strongly on the Pt surface in a wide range of potentials, resulting in a poor activity of platinum towards methanol electro-oxidation. This traduces in high oxidation overpotentials, usually far from the thermodynamic limit (E^0). Therefore, for commercial applications it is important to develop electro-catalysts tolerant to intermediate species. Good performance results have been obtained by combining Pt with oxophilic elements like Ru, Sn, Mo [4–8], because in the latter, the electro-dissociation of water that produces OH^- surface groups, occurs at lower potentials than on Pt

* Corresponding author. Tel.: +52 55 5622 5363; fax: +52 55 5550 1572.
E-mail address: roquero@servidor.unam.mx (P. Roquero).

0920-5861/$ – see front matter © 2005 Elsevier B.V. All rights reserved.
doi:10.1016/j.cattod.2005.07.106

alone. These OH groups oxidize the organic intermediate species, adsorbed at adjacent platinum sites, to CO_2. This phenomenon was denominated by Watanabe as the double catalytic effect [6,7]. It has also been suggested that the presence of the second metal can weaken the Pt–CO bond, resulting in higher tolerance of the catalyst towards CO poisoning.

Interesting results have been found by combining molybdenum with platinum. Shropshire [9] reported the adsorption of molybdates in a Pt black electrode and from linear polarization experiments, observed that the addition of Na_2MoO_4 to the electrolyte, before adding the fuel (HCHO or CH_3OH), resulted in a decrease of 0.3 V in the oxidation onset potential with respect to Pt. Cyclic voltammetry (CV) and differential electrochemical mass spectrometry (DEMS) experiments carried out on the CO oxidation reaction on Pt(1 1 1), Pt(3 3 2) and polycrystalline Pt materials with deposited Mo [10], revealed that CO presents two oxidation peaks. The first one around 0.55 V versus RHE, corresponding to the oxidation of weakly adsorbed CO, and a second one at 0.72 V versus RHE, resulting from the oxidation of strongly adsorbed CO. The presence of Mo caused a 0.15 V displacement of the first peak to lower potentials. According to the bifunctional mechanism, the intermediate Mo oxidation states (Mo(III) and Mo(IV)) work as donors of OH^- species. The Mo(VI) species do not seem to be efficient oxidants, since the peak corresponding to strongly adsorbed CO does not change in position. XPS allowed the identification of $MoO(OH)_2$ formation on Pt–Mo and Pt–Mo/C at about the same potentials of methanol oxidation [11]. Olivera et al. [12] found an insignificant decrease in the overpotential in the presence of Mo for the methanol oxidation reaction. However, the current density was higher, indicating good tolerance to the intermediate species. Pinheiro et al. [13] carried out experiments of ethanol oxidation, finding that the presence of Mo resulted in higher current densities than those found for methanol oxidation, showing that Mo helps to break the C–C bonding. It has also been reported that molybdenum does not present affinity towards CO and therefore, more sites on the Mo surface can be available over a wide range of potential to electro-dissociate water, contributing to the generation of OH^- species to oxidize organic intermediates adsorbed at adjacent Pt sites [14].

Considerable effort to develop catalytic materials tolerant to the intermediate species formed by the methanol oxidation reaction has been carried out. Pt–Mo/C materials seem to be good candidates. However in these materials, the electrochemical role of Mo is not clear. It has not been well established if molybdenum can work according to the double catalytic effect, or if methanol can be oxidized directly on the molybdenum surface. The purpose of the present work is to study the effect of Mo on Pt-Mo/C electrocatalysts obtained by a novel method based on the decomposition of Mo and Pt carbonyls. Electrochemical potential sweep techniques (cyclic voltammetry and rotating disk electrode) were used to investigate the oxidation of methanol on molybdenum, the possible existence of molybdenum hydroxides, and the promoting effect of this element on the reaction catalyzed by platinum.

2. Experimental

2.1. Synthesis of platinum carbonyls

The Pt carbonyl complex was synthesized by bubbling CO during 24 h at a volumetric flow rate of 25 cm^3/min through 50 cm^3 of an aqueous chloroplatinic acid solution (10 mg/cm^3 H_2PtCl_6). With the system under constant stirring, the color changed from orange to cherry red until a dark precipitate was obtained. These color changes correspond to different polymeric chains of Pt carbonyl complexes [15]. At the end of the reaction time, the stirring was stopped and the Pt carbonyl precipitate was filtered and dried under a CO atmosphere.

2.2. Synthesis of Pt-Mo/C catalysts

In accordance with the methodology proposed by Dickinson [16], the synthesis of Pt-Mo/C catalysts was carried out by placing the appropriate quantities of Pt carbonyl complex, molybdenum hexacarbonyl complex ($Mo(CO)_6$), and vulcan XC72R carbon in a reflux system using *o*-xylene as solvent. The system temperature was increased to the boiling point of *o*-xylene (140 °C) and reflux was maintained for 24 h. Once the selected contact time was reached, the solvent was distilled.

2.3. Prepared materials

Table 1 shows the different catalysts prepared by the method described above. All of them were formulated with 80 wt.% Vulcan carbon and 20 wt.% active phase. The composition of the active phase varied according to the atomic ratio $R = Mo/(Mo + Pt) = 0$, 0.2, 0.5, 0.8 and 1.

2.4. Fourier transform infrared spectroscopy (FTIR)

The Pt carbonyl complex was analyzed by FTIR. A sample of precipitate was dissolved in tetrahydrofurane

Table 1
Prepared materials

Prepared catalysts	Atomic relationship $R = \frac{Mo}{Mo+Pt}$	Pt:Mo relationship	Weight (%)		
			Pt	Mo	Carbon
Pt/C	0.0	1:0	20	0	80
Pt4Mo1/C	0.2	4:1	17.8	2.2	80
Pt1Mo1/C	0.5	1:1	13.4	6.6	80
Pt1Mo4/C	0.8	1:4	6.7	13.3	80
Mo/C	1.0	0:1	0	20	80

(THF) and placed between two CaF_2 monocrystals. The spectra were obtained using a Nicolet 510 FTIR spectrometer with a Michelson interferometer with a resolution of 2 cm^{-1}.

2.5. Electrochemical measurements

The working electrode was prepared by mixing graphite paste with 5 mg of the catalyst to be analyzed, and placing it on the surface of a 0.5 cm diameter graphite rotating disk electrode (RDE). The geometric surface area of the disk was used for the calculation of current density. The different working solutions consisted of 1.0 M methanol, 1.0 M formaldehyde, and 1.0 M formic acid, all of them with 0.5 M H_2SO_4 as supporting electrolyte. Before carrying out the tests, the solutions were purged with argon for 15 min.

The electrochemical experiments were carried out at 25 °C using a Radiometer Voltalab 50 potentiostat-galvanostat. A three-electrode cell was used with a saturated calomel electrode (SCE:Hg/Hg_2Cl_2 /sat. KCl) as reference and a platinum wire as counter electrode. All potentials reported in this work are referred to the reversible hydrogen electrode. For the cyclic voltammetry measurements the system was kept without stirring. All the potential sweeps in CV were first carried out towards positive potentials, and then reversed towards negative potentials. For the rotating disk electrode technique, the rotation speeds were 300, 700, 1100 and 1500 rpm and the potential sweep rate was 5 mV/s. In some cases, before performing the RDE scans, a constant potential was applied to the electrode in order to reduce or oxidize the catalyst material and facilitate the identification of anodic or cathodic processes in the potential sweep.

2.6. X-ray diffraction (XRD)

Diffractograms were obtained at room temperature using Cu Kα (λ = 1.5406 Å) radiation on a Siemens D-500 diffractometer, with a speed of 2° min^{-1}.

2.7. Transmission electronic microscopy (TEM)

The samples were dispersed in *n*-heptane, in an ultrasound bath for 1 h. Some drops of the supernatant liquid were deposited on 200-mesh copper grids covered with a carbon film. Images were obtained with a JEOL 2010 microscope. Particle size distribution was obtained from the evaluation of 266 particles from 10 different images.

3. Results and discussion

Fig. 1 shows the infrared spectra of Pt carbonyl dissolved in THF. The band at 2057–2060 cm^{-1} corresponds to terminal carbonyls, while the band at 1869–1879 cm^{-1} is associated to the bridge carbonyl group. In accordance to the position of the peak maximum, the Pt carbonyl polymer obtained, $[Pt_3(CO)_3\ (\mu_2\text{-}CO)_3]_n^{2-}$, has $n = 5$, where n represents the monomeric units in the polymer [15]. The band at 1970 cm^{-1} corresponds to the THF solvent, and disappears as it evaporates. The change in the width of the band corresponding to the terminal carbonyl group, around 2057 cm^{-1}, can be explained by the presence of Pt carbonyl polymer chains with different molecular weight.

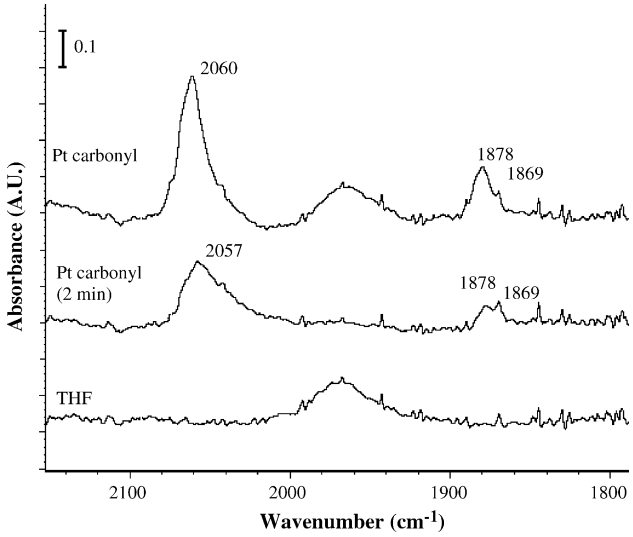

Fig. 1. FTIR determinations for the Pt carbonyl complex.

Fig. 2 presents the TEM image of Pt/C. This material shows a uniform distribution of small particle sizes, mainly between 1 and 3 nm. The Pt4Mo1/C catalyst (Fig. 3), presents a homogeneous dispersion with similar particle sizes (3 nm). The other synthesized materials display similar characteristics.

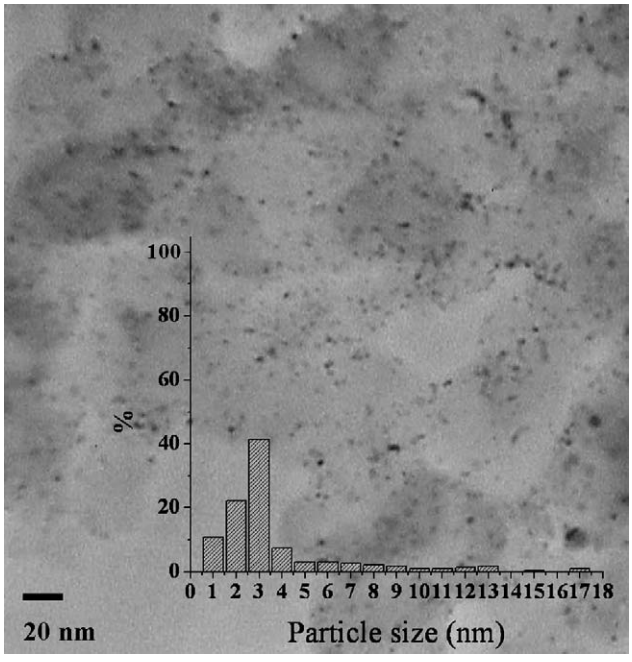

Fig. 2. TEM image of Pt/C.

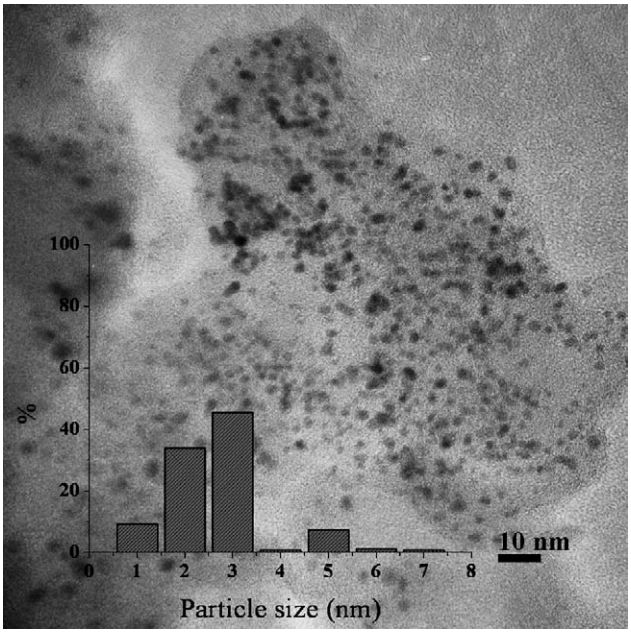

Fig. 3. TEM image of Pt4Mo1/C.

In the X-ray diffraction pattern for the Pt–Mo/C series, shown in Fig. 4, diffraction lines that correspond to the (1 1 1), (2 0 0), (3 1 1), and (2 2 2) planes of metallic platinum (card 4-0802) are evident. The intensity of these lines increase with the Pt content in the formulation. Vulcan carbon has the characteristics of graphitic carbon. The Mo/C sample presents a pattern similar to that of Vulcan carbon.

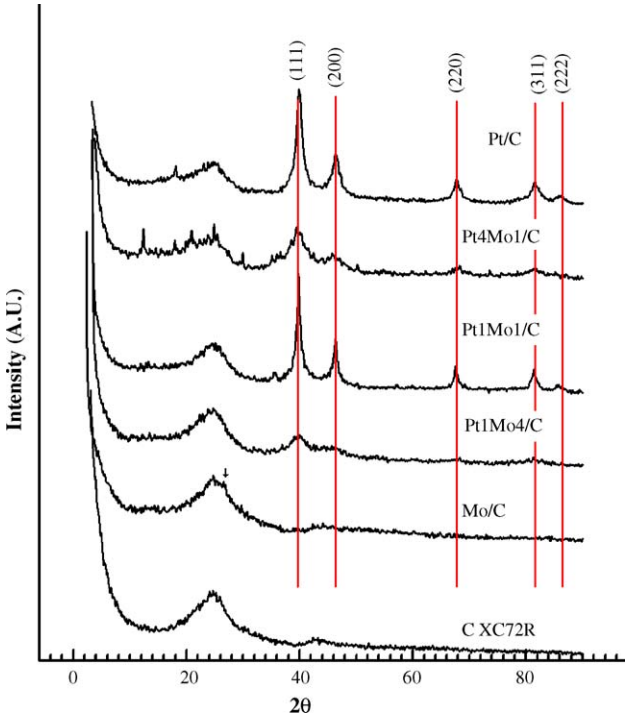

Fig. 4. XRD of Pt–Mo/C series.

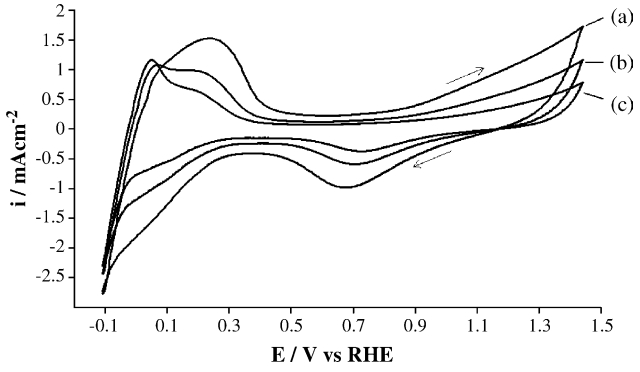

Fig. 5. Cyclic voltammograms of Pt/C in H_2SO_4 0.5 M at several scan rates: (a) 200 mV/s; (b) 100 mV/s; (c) 50 mV/s.

However, at $2\theta = 26^\circ$ a peak that can be attributed to MoO_3 is found.

Fig. 5 presents the voltammograms of the Pt/C catalyst in 0.5 H_2SO_4 at different sweep rates: 50, 100 and 200 mV/s. In the anodic scan, from −0.05 to 1.45 V versus RHE, the desorption of weakly and strongly adsorbed protons on different Pt planes, with peaks at 0.07 and 0.22 V versus RHE, respectively, is observed. At potentials higher than 0.5 V versus RHE the anodic current corresponding to oxygen electro-sorption and $Pt(OH)_2$ formation is observed, in agreement with the potentials reported by Pourbaix [17]. During the reverse sweep, the onset potential for the reduction of $Pt(OH)_2$ to metallic Pt is found at 1.076 V versus RHE.

Fig. 6 shows the voltammogram of the Mo/C electrocatalyst in 0.5 M of H_2SO_4. It is not possible to distinguish proton adsorption and desorption processes. Several peaks at 0.13, 0.32, 0.69 and 1.03 V versus RHE are found in accordance with potential–pH diagrams for Mo [14]. These peaks are due to changes in the oxidation state of molybdenum from 0 to VI. The peaks that appear in the scan towards the negative potentials are due to reduction of Mo(VI)–Mo(0). Some of the Mo species in oxidation states III or IV could be dissolved by the electrolyte in a corrosion process; however, after carrying out several cycles, the peak position and current intensities remained constant, indicating that the metal-support bond maintains the Mo species anchored to the surface.

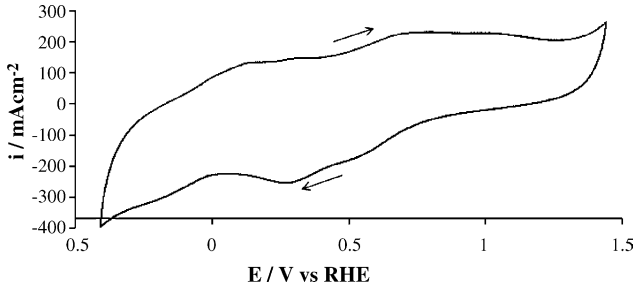

Fig. 6. Cyclic voltammogram of Mo/C in 0.5 M H_2SO_4 at 50 mV/s.

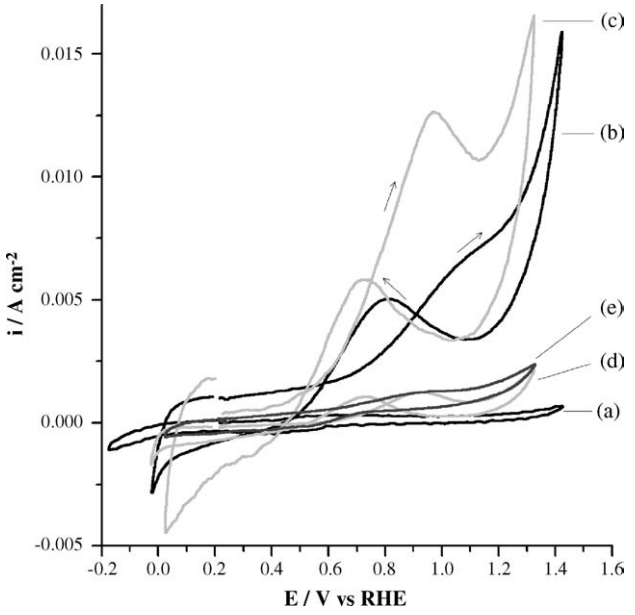

Fig. 7. Cyclic voltammograms of the catalysts series in 1.0 M CH_3OH, 0.5 M H_2SO_4 at 50 mV/s. (a) Mo/C; (b) Pt/C; (c) Pt4Mo1/C; (d) Pt1Mo1/C; (e) Pt1Mo4/C.

Fig. 7 presents the CV results for the whole Pt–Mo/C series. These experiments were recorded with a 50 mV/s scan rate, in a 1.0 M methanol, 0.5 M H_2SO_4 solution. For the Mo/C sample, no methanol oxidation peak was registered; only changes in Mo oxidation state are detected. In the scan towards positive potentials, the Pt/C electrocatalyst presents the methanol oxidation peak in the potential range of 0.9–1.2 V versus RHE. In the reverse scan, anodic currents are observed between 1.1 and 0.5 V. The slope change for this process is very marked and it is characteristic of the oxidation of adsorbed organic species. This anodic current starts at a potential very close to that for $Pt(OH)_2$ reduction in H_2SO_4 medium (Fig. 5). When the potential diminishes and the oxidation state of Pt changes from II to 0, the desorbed oxygen can participate in the oxidation of the intermediate organic species to CO_2. From the results of the entire series, it is evident that Pt4Mo1/C presents the lowest onset potential (0.38 V versus RHE against 0.5 V versus RHE for Pt/C) and the highest current density for the methanol oxidation reaction. Consequently, Pt4Mo1/C presents the highest methanol electro-oxidation activity. This result suggests that the maximum promoting effect is obtained with a low molybdenum content (4 wt.%)

Fig. 8 shows voltammograms for the Mo/C, Pt/C and Pt4Mo1/C catalysts in 1.0 M formaldehyde and 0.5 M H_2SO_4. The anodic current for organics oxidation in the forward scan is small, and rises at potentials >0.8 V versus RHE. In the reverse scan, the oxidation of adsorbed organics begins at the same potential as in the case of methanol (0.9 V versus RHE), and two oxidation steps are observed in this peak.

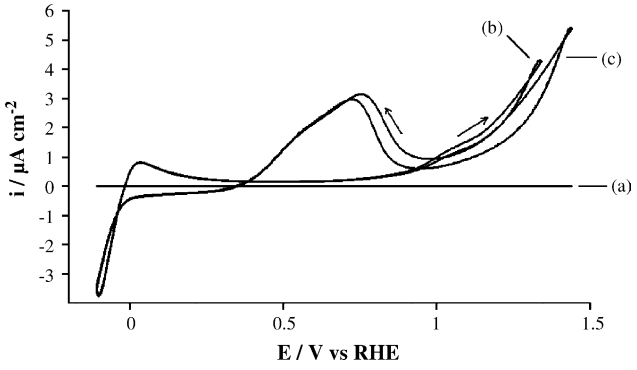

Fig. 8. Cyclic voltammograms of: (a) Mo/C; (b) Pt/C, and (c) Pt4Mo1/C in 1.0 M HCHO, 0.5 M H_2SO_4 at 50 mV/s.

Fig. 9 presents the voltamograms for Mo/C, Pt/C and Pt4Mo1/C in 1.0 M formic acid, 0.5 M H_2SO_4. These curves show in the forward scan that the anodic current rises at a potential of 0.5 V versus RHE and reaches a maximum at 1.1 V versus RHE. The total current density obtained was much lower than for methanol oxidation (Fig. 7). This occurs also for the anodic current in the reverse peak, which is sharper than the corresponding peaks in the methanol and formaldehyde media. So, it appears that formic acid and formaldehyde adsorb on the surface of Pt at lower electrode potentials than methanol.

With the rotating disk electrode experiments it is possible to distinguish the electrode reactions that are associated to diffusion processes from those that correspond to oxidation or reduction of the electrode material. When the current density varies with rotation speed, the process can be assumed to be influenced by diffusion [18]. The RDE curves for Mo/C presented in Fig. 10(a) are obtained from a potential sweep from low to high potentials (from −0.4 to 1.5 V versus RHE), after applying a cathodic pre-treatment consisting in the application of a constant potential of −0.4 V versus RHE, during 5 min. The purpose of this pre-treatment is to reduce the electrode, to evidence the oxidation of the material in the scan that follows, towards positive potentials. Fig. 10(b) shows the results for Mo/C with anodic pre-treatment: a potential step in 1.0 V versus

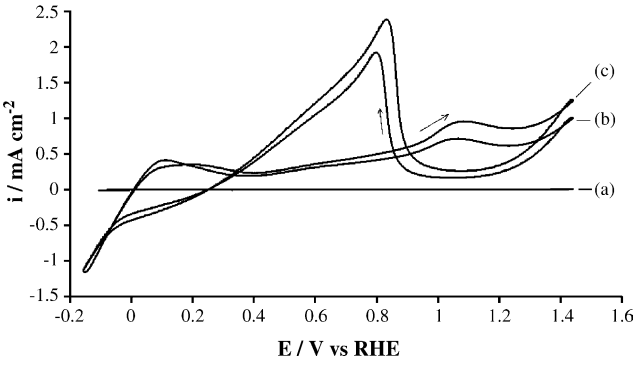

Fig. 9. Cyclic voltammograms of: (a) Mo/C; (b) Pt/C, and (c) Pt4Mo1/C in 1.0 M HCOOH, 0.5 M H_2SO_4 at 50 mV/s.

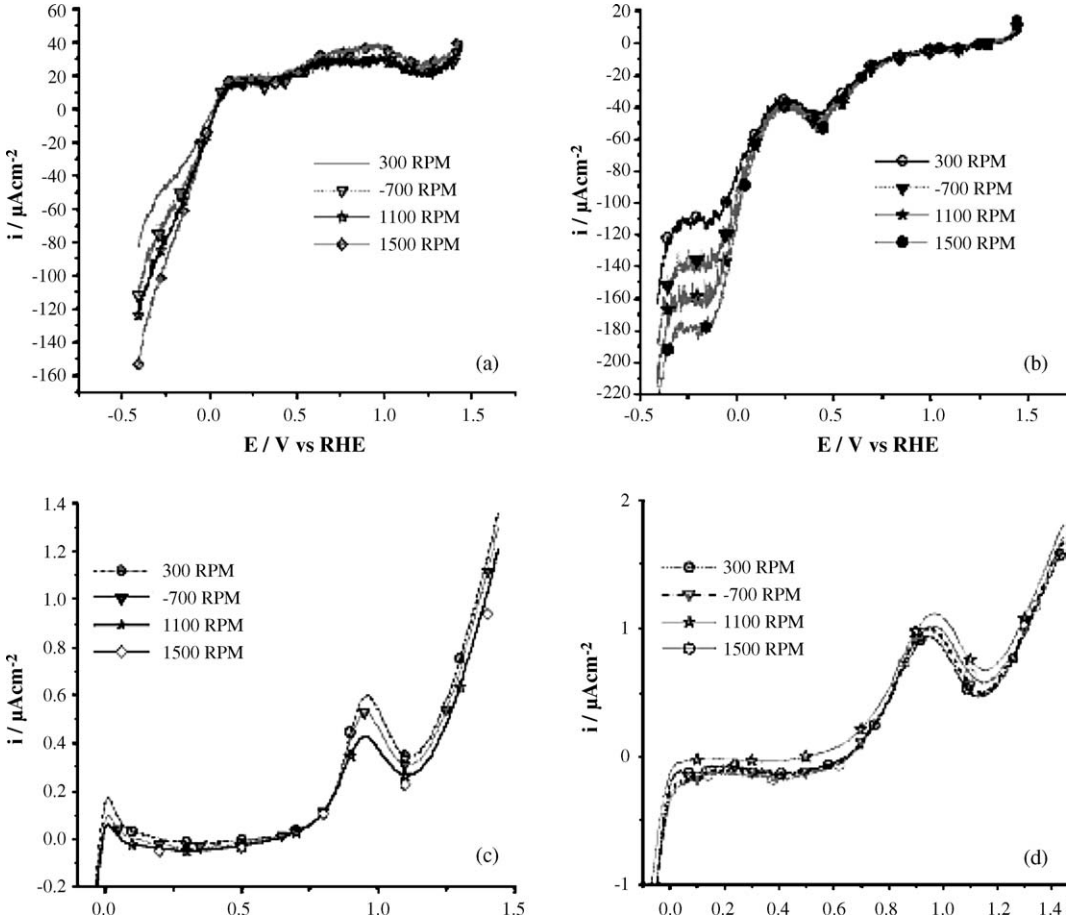

Fig. 10. Rotating disk electrode experiments in 1.0 M CH_3OH, 0.5 M H_2SO_4, for (a) Mo/C, cathodic pre-treatment; (b) Mo/C, anodic pre-treatment; (c) Pt/C, and (d) Pt4Mo1/C.

RHE was applied during 5 min, previous to the potential sweep from 1.5 to −0.4 V versus RHE. In these curves (Fig. 10(a) and (b)) it is possible to recognize that, at potentials lower than 0.2 V versus RHE, the reduction reaction that occurs in the electrode–electrolyte interface involves species that diffuse from the electrolyte. These species are protons that can form molybdenum hydroxides. In the anodic sweep (Fig. 10(b)) the diffusion plateau for this reduction is clearly established between −0.12 and −0.36 V versus RHE. At potentials lower than −0.36 V versus RHE the reduction current density increases because of the hydrogen evolution reaction. In the potential range between 0.2 and 1.5 V versus RHE the current density does not change significantly with rotation speed, therefore, it can be concluded that oxidation (Fig. 10(a)) and reduction (Fig. 10(b)) reactions in this potential interval are only due to changes in the oxidation state of molybdenum. No oxidation current is observed for methanol oxidation.

Fig. 10(c) and (d) show the scans towards positive potentials without pre-treatment, for the Pt/C and Pt4Mo1/C catalysts in methanol. Here the only diffusion process that can be identified is that of methanol oxidation at potentials between 0.8 and 1.15 V versus RHE.

4. Conclusions

From the above results it can be concluded that in Pt-Mo/C electro-catalysts, molybdenum has only a promoting effect, and does not participate directly as catalyst in the methanol electro-oxidation. The increment in the activity of the catalyst can be related to the change in the oxidation state of Mo(IV)–Mo(VI).

The highest promoting effect towards methanol electro-oxidation is obtained at low Mo contents like in the case of Pt4Mo1/C. This promoting effect manifests itself as a change in the oxidation onset potential to lower values than in Pt/C.

Diffusion-controlled currents, observed in the RDE experiments, show that molybdenum can form hydroxides at potentials lower than 0.2 V versus RHE. Mo-OH species can react with Pt-CO and other organic intermediates to produce CO_2. However, it is not certain that these OH groups exist on the surface of molybdenum at the potentials for methanol oxidation (about 0.6 V versus RHE). Moreover, no anodic currents and no diffusion processes, associated to methanol oxidation are observed on Mo/C.

The synthesis method based on the thermolysis of metal carbonyls produces high dispersion of the metallic particles

over the support surface, providing small particle sizes between 2 and 3 nm.

The catalyst active phase is stable since no corrosion currents are observed during potential sweeps or potential steps.

Acknowledgements

The authors wish to express their gratitude to Professor Martín Hernández Luna for his continuing support in this research, to Dr. Aída Gutiérrez Alejandre for the realization of FTIR measurements to Mr. Iván Puente Lee for the TEM images and to Mr. Manuel Aguilar Franco for the XRD analysis.

References

[1] Y. Zhu, H. Uchida, T. Yajima, M. Watanabe, Langmuir 17 (2001) 146.
[2] H. Xia, T. Iwasita, F. Ge, W. Vielstich, Electrochim. Acta 41 (1996) 711.
[3] Y.C. Liu, X.P. Qiu, Y.P. Huang, W.T. Zhu, Carbon 40 (2002) 2375.
[4] M. Götz, H. Wendt, Electrochim. Acta 43 (1998) 3637.
[5] T. Frelik, W. Visscher, J. Van Veen, Surf. Sci. 335 (1995) 353.
[6] M. Watanabe, S.J. Motoo, J. Electroanal. Chem. 60 (1975) 267.
[7] M. Watanabe, S.J. Motoo, J. Electroanal. Chem. 60 (1975) 275.
[8] H. Nakajima, H. Kita, Electrochim. Acta 35 (1990) 849.
[9] J.A. Shropshire, J. Electrochem. Soc., May (1965) 465.
[10] G. Samjeske, H. Wang, T. Löffler, H. Baltruschat, Electrochim. Acta 47 (2002) 3681.
[11] B.N. Grgur, N.M. Markovik, P.N. Ross, J. Electrochem. Soc. 146–5 (1999) 1613.
[12] A. Oliveira Neto, E.G. Franco, E. Arico, H. Linardi, E.R. Gonzalez, J. Eur. Ceramic Soc. 23 (2003) 2987.
[13] A.L.N. Pinheiro, A. Oliveira, E.C. Souza, J. Perez, V.A. Paganin, E.A. Tiaccinelli, E.R. González, J. New Mater. Electrochem. Syst. 6 (2003) 1.
[14] S. Mukerjee, R.C. Urian, Electrochim. Acta 47 (2002) 3219.
[15] G. Longini, P. Chini, J. Am. Chem. Soc. 98 (23) (1976) 10.
[16] A.J. Dickinson, L.P. Carrette, J.A. Collins, K.A. Friedrich, U. Stimming, Electrochim. Acta 47 (2002) 3733.
[17] M. Pourbaix, Atlas D'Équilibres Électrochimiques, Gauthier Villars Éditeur, Paris, 1963.
[18] R. Greef, R. Peat, L.M. Peter, D. Pletcher, J. Robinson, Instrumental Methods in Electrochemistry, Ellis Horwood, UK, 1990.